Article

Not peer-reviewed version

Carbonization of Refuse-Derived Fuel Pellets with Biomass Incorporation to Solid Fuel Production

Andrei Longo *, Nuno Pacheco, Roberta Mota-Panizio *, Cândida Vilarinho, Paulo Brito, Margarida Gonçalves

Posted Date: 27 June 2024

doi: 10.20944/preprints202406.1905.v1

Keywords: Refuse-Derived Fuel; Pelletization; Dry carbonization; Hydrothermal carbonization

 doi:10.20944/preprints202406.1905.v1

Article

Carbonization of Refuse-Derived Fuel Pellets with Biomass Incorporation to Solid Fuel Production

Andrei Longo [1,*], Nuno Pacheco [2], Roberta Panizio [1,3,*], Cândida Vilarinho [2,4], Paulo Brito [1] and Margarida Gonçalves [1,3]

[1] VALORIZA — Research Centre for Endogenous Resource Valorization, Portalegre Polytechnic University, Campus Politécnico 11, 7300-555 Portalegre, Portugal.
[2] CVR — Center for Waste Valorization, University of Minho, 4800-058 Guimarães, Portugal.
[3] MEtRICs — Mechanical Engineering and Resource Sustainability Center, NOVA School of Science and Technology (FCT NOVA), NOVA University of Lisbon, Campus Caparica, 2829-516 Caparica, Portugal.
[4] MEtRICs — Mechanical Engineering and Resource Sustainability Center, Mechanical Engineering Department, School of Engineering, Minho University, Campus de Azúrem, 4800-058 Guimarães, Portugal.
* Correspondence: andrei.longo@ipportalegre.pt; rpanizio@ipportalegre.pt

Abstract: In this work, dry and hydrothermal carbonization (DC and HTC) of RDF pellets were conducted to evaluate the physical, chemical, and fuel properties of the produced chars. In the dry carbonization tests, biomass sawdust was incorporated in different proportions on the samples to minimize agglomeration caused by the melting of the plastic fraction. The experiments were carried out in a temperature of 400°C (DC) and 250-300°C (HTC), in a residence time of 30 minutes. The respective chars and hydrochars were characterized according to their mass yield, apparent density, proximate, elemental, and mineral composition, chlorine content, high heating value, thermogravimetric profile, and surface functional groups. The results showed that dry carbonization of RDF pellets with biomass incorporation, followed by a washing step, resulted in the production of chars with improved properties such as higher fixed carbon and HHV (25-26 MJ/kg) and lower ash and chlorine content. Additionally, the HTC experiments demonstrated that hydrochars showed improved properties without the need for biomass addition and washing, however, with no significant difference in the HHV (20-21 MJ/kg). Therefore, DC of RDF pellets with 10% biomass incorporation seems to be a promising option to overcome the constraints of RDF utilization as an alternative fuel.

Keywords: refuse-derived fuel; pelletization; dry carbonization; hydrothermal carbonization

1. Introduction

Energy recovery from waste is an established strategy for reducing the amount of waste sent to landfills while simultaneously generating energy from alternative resources [1]. In the last decades, several works had focused on improve waste valorization techniques to produce alternative fuels more efficently and minimize the associated environmental impacts [2–4]. However, the production of solid fuels with higher energy content, improved fuel properties and lower levels of pollutants remains an ongoing challenge in the domain of waste utilization. Several factors such as high heterogeneity, high moisture content, ash content, and the presence of contaminants, play significant roles that can hinder or altogether obstruct the transformation of waste into a viable energy source [5,6].

RDF production is an efficent strategy to improve municipal or industrial residues characteristics by selecting the high calorific fraction for energetic purposes [7]. Even though the RDF approach enhances the homogeneity and reduces moisture content when compared to the raw material, the combustion of this waste fraction leads to technical issues regarding the different combustion behavior of its components, as well as the emission of chlorine species from the plastic fraction [8].

 doi:10.20944/preprints202406.1905.v1

To address these challenges, it is essential to subject the waste to various pre-treatments to enhance its physical properties or combustible characteristics, rendering it a potential alternative to fossil fuel sources [9].

The carbonization of waste as pre-treatment for the production of alternative fuels with attractive characteristics to be used in combustion or gasification is justified by the improvement of the physical properties and/or fuels of biomass or residue, associated with increased economic efficiency and reduction of associated environmental impacts [10]. Furthermore, the co-carbonization of different waste fractions plays a significant role in improving energetic waste valorization, since it can overcome some physical and chemical constraints reported during thermochemical valorization processes [11–14]. The combined effect of the co-carbonization of different waste streams may enhance the chars' properties and increase the process efficiency [15]. Rago et al. [16] concluded that the synergistic effect of the co-carbonization of biomass and plastic intensified the increase in calorific value and maximized the mass yield of biochars since the melting of plastics inhibited mass transfer during co-carbonization with biomass. Similarly, Shen et al. [17] and Yao and Ma [18] found that combining biomass and plastics with high chlorine content enhances dechlorination efficiency and improves fuel properties.

In addition to using thermochemical recovery methods, densification of RDF offers significant logistical benefits, which can play a crucial role when deciding on the most suitable waste energy recovery method. Although the densification of raw biomass has already been widely described as a method that enhances the energy recovery logistics of this material [19,20], the densification of MSW or RDF presents a challenge. Unlike biomass, which contains lignin serving as a natural binding agent, additional components are often required for efficient pelletization. This constraint can potentially impact the technical and economic feasibility of the RDF pelletization process [22]. Zaini et al. [23] reported that the presence of lignin in the RDF composition increased mechanical resistance and played a crucial role in the stability of pellets during the pyrolysis process. The co-pelletization of RDF with pine biomass in the form of sawdust in different proportions was described by García et al. [24], as a viable process for producing alternative fuels suitable for industrial use.

Moisture content and particle size are important factors that affect the efficiency of RDF densification. According to Rezaei et al. [25], having moisture levels below 20% in the material increases the amount of energy needed for pelletization, while higher values can decrease the durability and mechanical resistance of the pellets. Sprenger et al. [22] found that the optimal production of RDF pellets occurs with 15% moisture and approximately 20% ash content. Some studies have shown that using thermochemical methods along with densification can enhance the properties of pellets produced from biomass residues [26–29]. Regarding RDF, reducing the particle size and achieving a more uniform distribution of char particles can lower the energy required for crushing. However, the reduced proportion of this fraction in RDF composition makes it challenging for lignin to bind the waste particles, needing the use of binding agents which increases the process costs [30] and the moisture absorption capacity [31], leading to a decreased in the calorific value of the material.

This work aims to assess the physical, chemical, and fuel properties of pellets produced from RDF after undergoing dry and hydrothermal carbonization processes aiming at the production of high-quality solid biofuel.

2. Material and Methods

2.1. Refused-Derived Fuel Pellet Sample

The carbonization tests in this work were carried out with a pelletized RDF sample, supplied by the Waste Recovery Center (CVR), produced from municipal solid wastes (Figure 1a). For the dry carbonization tests, lignocellulosic biomass waste (LBW), mainly pine waste from furniture recycling, was supplied by CMC Biomass S.A., a biomass waste management company. The waste was used in sawdust form with a particle size smaller than 5 mm (Figure 1b).

 doi:10.20944/preprints202406.1905.v1

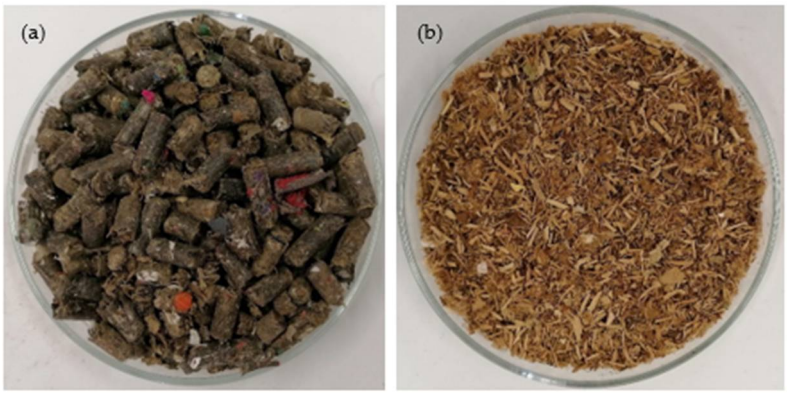

Figure 1. RDF pellets and biomass used in the carbonization tests.

The RDF sample used in the pellets production was provided by Braval, S.A., a Portuguese waste management company. This waste is composed of plastics (28.7 ± 3.0%), textiles (22.9 ± 3.9%), paper/cardboard (15.1 ± 3.7%), wood (2.6 ± 0.4%), aluminum (2.4 ± 0.3%), and miscellaneous particles (30.8 ± 2.6%). The miscellaneous corresponds to a mixture of all fractions with low granulometry. The aluminum fraction was removed manually from the samples before the carbonization tests. The produced RDF pellets had 12.6% of moisture content, 97.7% of mechanical durability and 0.3% of fine particles.

2.2. Carbonization Tests

The dry carbonization tests were conducted at a temperature of 400°C in a muffle furnace (Kilper®, CK 25-E) with a capacity of 80L. The residues were carbonized in covered porcelain crucibles with a capacity of 250 mL for a residence time of 30 minutes and removed from the muffle 30 minutes after turning it off. The experiments were carried out using RDF pellets samples alone and with 10% and 25% biomass incorporation. The aim of incorporating biomass was to reduce particle agglomeration caused by the melting of the plastic fraction and to assess any physical, chemical, and fuel enhancements in the produced char.

The hydrothermal carbonization tests were conducted using only RDF pellets, without the inclusion of biomass. The tests were performed at temperatures of 250°C and 300°C, with solid-liquid (S/L) ratios of 1:2.5 and 1:5. The purpose was to assess the impact of raising the temperature and the amount of liquid in the reactor on the physical, chemical, and fuel properties of the hydrochars. After the test, the reactor was allowed to cool to room temperature and then carefully opened to release internal pressure. The material was then filtered to separate the hydrochars and HTC effluent. The hydrochars were dried in a stove (Memmert®) at 105°C for 24 hours, and the liquid fraction was stored for further analysis. Table 1 summarizes the carbonization conditions for both dry and hydrothermal experiments conducted in this study.

Table 1. Sample composition and carbonization conditions.

Thermochemical process	Sample	Sample composition (%)		S/L ratio	T (°C)	t (min.)
		RDF	Biomass			
Dry carbonization (DC)	100P	100	-	-	400	30
	90P10B	90	10	-		
	75P25B	75	25	-		

 doi:10.20944/preprints202406.1905.v1

Hydrothermal carbonization (HTC)	100P	100	-	1:2.5	250	30
				1:5	300	

2.3. Chars Characterization and Fuel Properties

The chars and hydrochars produced under various carbonization conditions were characterized based on their physical, chemical, and fuel properties. These properties included mass yield (Eq.1), apparent density (Eq.2), proximate composition (CEN/TS 15414-3:2010, EN 15402:2011 and EN 15403:2011, for moisture, volatile matter and ash content, respectively), elemental composition (Thermo Finnigan—CE Instruments Model Flash EA 112 CHNS series, San Jose, CA, USA), ash mineral composition (ICP-AES, Horiba Jobin-Yvon Ultima, France), chlorine content (Thermo Scientific Niton XL3t GOLDD + XRF analyzer, Waltham, MA, USA), and high heating value (calorimeter IKA® C200, Staufen, Germany).

The fouling and slagging index of the ashes were calculated using some indicators such as the base/acid ratio (B/A), bed agglomeration index (BAI), fouling index (Fu), slag tendency based on the silica/alumina ratio (S/A) and total alkali (TA), according to Ovcacíková et al. [32].

$$Mass\ yield\ (\%, db) = \frac{m_{char}}{m_{raw}} \times 100 \qquad \text{Eq. (1)}$$

$$Apparent\ density\ (\%, db) = \frac{m_{char}}{v_{char}} \qquad \text{Eq. (2)}$$

where m_{char} and v_{char} are the mass and volume of the chars; m_{raw} is the mass of raw RDF pellet samples.

In addition, structural analysis by FTIR (Nicolet 174 iS10 FT-IR Spectrometer, Madison, WI, USA) and thermogravimetric profile (Q50 TG, TA Instruments, New Castle, DE, USA) were carried out. The ignition and burnout temperatures are calculated according to the interception method described by Liu et al. [33].

2.4. Char Washing and Effluent Characterization

The char washing process was carried out according our previous work [34]. In brief, the chars produced through dry carbonization were washed in hot distillated water in a S/L ratio of 1:5 in open beakers, until reaching the boiling point. Thereafter, the sample were left to cool at room temperature and filtered to separate the solid and liquid fractions. The chars were then placed in a muffle at 105°C for 24h to dry, and the wastewater was stored to further characterization.

The wastewater from the chars washing and the liquid effluent resulting from the HTC tests were analyzed for pH, chemical oxygen demand (COD), chloride concentration, as well as the amount of total, volatile, and fixed solids (ash). The pH was measured using a pH meter (Crison MicropH 2001 meter, Spain). Total solids and COD were evaluated using methods 2540B and 5220B of the Standard Methods for the Examination of Water and Wastewater, respectively. The chloride content was evaluated using the titration method according to the methodology described in EPA-SW-948, test method 9253. All measurements were carried out in triplicate, and the results presented correspond to average values. Ash composition was accessed through ICP-AES (as described for chars).

3. Results and Discussion

3.1. Carbonization Tests and Char's Characterization

During the dry carbonization process, it was observed that the sample consisting solely of RDF pellets exhibited greater particle aggregation, which gradually decreased with the addition of biomass. Under all conditions tested, the chars showed a dark and homogeneous color. The mass yield of the chars decreased as the amount of biomass in the sample increased (Figure 2a). The char

 doi:10.20944/preprints202406.1905.v1

produced by RDF pellets without biomass incorporation had a mass yield of 66%, whereas the yield decreased to 57.3% with greater biomass incorporation. The sample with 10% biomass had an average mass yield of 65.2%. Additionally, the apparent density of the chars gradually decreased as the biomass content increased. For the sample composed only of RDF pellets, the apparent density was 0.607 g/cm^3, which is an 11.5% decrease compared to the raw RDF pellets (0.686 g/cm^3). In samples with 10% and 25% biomass content, the apparent density decreased to 0.593 g/cm^3 and 0.572 g/cm^3, respectively.

The hydrochars produced from RDF pellets had a homogeneous appearance and a dark color that varied depending on the temperature applied. The samples produced at 250°C had more agglomerates and a slightly lighter brown color compared to the samples produced at 300°C, which had a smaller particle size and a black color. As the carbonization temperature rises, there was a corresponding decrease in hydrochar yield (Figure 2b), consistent with previous research [35]. Additionally, increasing the S/L ratio was found to have a negative impact on mass yield. The highest yield was achieved at a temperature of 250°C with an S/L ratio of 1:2.5 (69.3%). Conversely, the lowest yield was observed at a temperature of 300°C with an S/L ratio of 1:5 (59.3%).

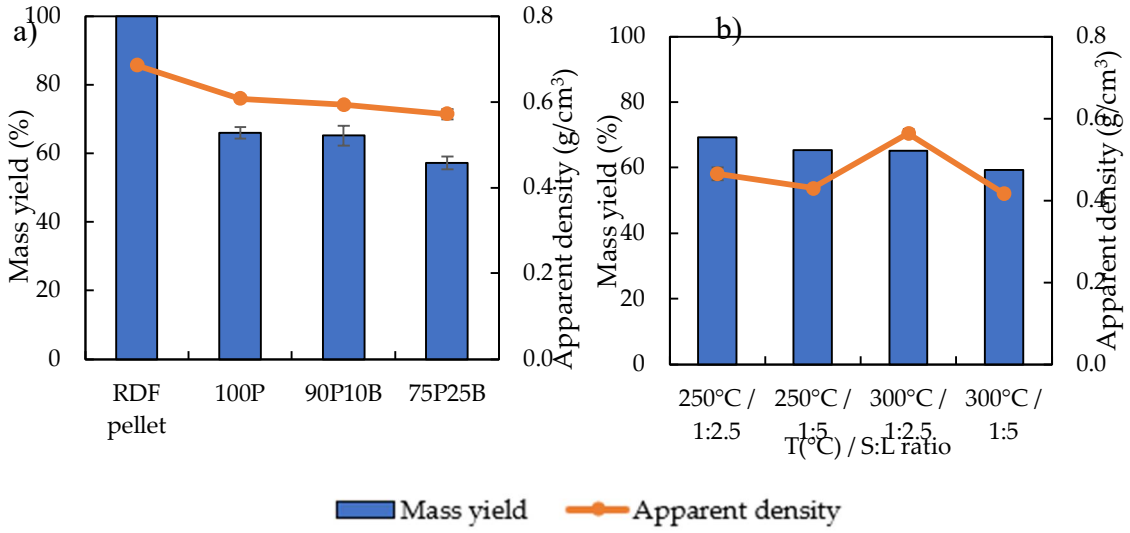

Figure 2. Mass yield and apparent density of the chars (a) and hydrochars (b).

The increase in carbonization temperature from 250°C to 300°C had a greater impact on increasing the apparent density at an S/L ratio of 1:2.5, but this behavior was not observed at 1:5. Additionally, increasing the S/L ratio seemed to have a negative effect on the value at 250°C. The hydrochars with the highest apparent density were produced at 250°C in an S/L ratio of 1:2.5 (0.564 g/cm^3), while the lowest value was observed in hydrochars produced at the same temperature but in an S/L ratio of 1:5 (0.417 g/cm^3). The samples produced at 300°C had values of 0.430 g/cm^3 at the S/L ratio of 1:2.5 and 0.465 g/cm^3 at the S/L ratio of 1:5.

The proximate composition of the raw RDF, chars and hydrochars is detailed in Table 2. The moisture content of samples without the addition of biomass averaged 2.5%, increasing to 3.0% with the inclusion of 10% biomass. However, when the biomass content was increased to 25%, the moisture content reduced to 2.6%, indicating a non-uniform pattern in relation to the biomass addition. Carbonization led to the production of more hydrophobic chars with lower moisture content compared to the raw waste. Additionally, the process release moisture and volatile matter from the raw waste, which leads to higher fixed carbon in chars, especially in the dry carbonization process.

Table 2. Proximate composition of the raw wastes, chars and hydrochars.

Sample	Proximate composition (%)

 doi:10.20944/preprints202406.1905.v1

	Moisture	Volatile matter*	Ash*	Fixed carbon*
Raw RDF pellet	12.6 ± 0.3	76.9 ± 3.7	15.9 ± 1.1	7.2 ± 2.9
LBW	10.7 ± 0.2	76.0 ± 1.0	6.2 ± 0.5	17.8 ± 1.4
100P	2.5 ± 0.1	63.1 ± 1.3	26.3 ± 0.7	10.6 ± 1.5
90P10B	3.0 ± 0.1	60.8 ± 1.0	25.0 ± 0.3	14.2 ± 1.2
75P25B	2.6 ± 0.1	55.2 ± 0.6	21.6 ± 0.4	23.1 ± 0.8
100P 250°C 1:2.5	2.7 ± 0.0	70.1 ± 1.3	22.5 ± 1.4	7.0 ± 2.2
100P 250°C 1:5	1.8 ± 0.0	72.8 ± 1.0	21.0 ± 1.7	6.2 ± 0.6
100P 300°C 1:2.5	1.9 ± 0.1	70.6 ± 2.5	17.2 ± 2.2	13.3 ± 0.8
100P 300°C 1:5	2.7 ± 0.0	71.4 ± 0.9	20.3 ± 0.5	8.3 ± 1.2

*In a dry basis.

The volatile matter and ash contents decreased with the increase in the percentage of biomass in the samples due to the greater devolatization of this fraction at the applied carbonization temperature (400°C) and the higher ash content present in the RDF components compared to biomass [36]. Consequently, the sample without biomass had the highest value of volatile matter in chars (63.1%), while the sample with the highest biomass content exhibited the lowest value (55.2%). Char produced with 10% biomass showed an intermediate value (60.8%). The ash content exhibited the same trend, with the highest value of 26.3% found in the RDF pellet char sample and gradually decreasing to average values of 25% and 21.6% in samples with 10% and 25% biomass incorporation, respectively. The fixed carbon content raised proportionally to the increase in biomass incorporation into the sample. Adding 10% biomass led to a 33.4% increase in fixed carbon content, from 10.6% to 14.2%. With 25% biomass incorporation, the fixed carbon content more than doubled compared to the sample without biomass, reaching 23.1%.

Regarding the hydrochars, it was observed that the moisture content is affected by both temperature and the S/L ratio. Higher temperatures and S/L ratios were seen to reduce moisture content, with the lowest value of 1.6% observed in hydrochars produced at 300°C with an S/L ratio of 1:5. Conversely, the highest moisture content at 2.7% was found in samples at 250°C with the same S/L ratio. When considering volatile matter, the S/L ratio had a more significant effect than temperature. An increase in volatile matter was noticed in samples with a 1:5 S/L ratio, with percentages of 72.8% and 71.4% for hydrochars produced at 250°C and 300°C, respectively.

The ash content did not showed a consistent pattern, with 250°C samples ranging from 21.0 to 22.5%, and the lowest percentage occurring at an S/L ratio of 1:5. At 300°C, the trend was reversed, with the lowest ash content at 17.2% in the 1:2.5 S/L ratio sample, which then increased to 20.3% at a 1:5 ratio. As the carbonization temperature rose, there was a corresponding increase in fixed carbon content, which was inversely related to the S/L ratio. For example, hydrochars produced at 300°C with a 1:2.5 S/L ratio had an average fixed carbon content of 13.6%, while those produced at 250°C with a 1:5 ratio had only 6.1%.

The elemental composition of the raw wastes, chars, and hydrochars is showed in Table 3. Both carbonization processes increased the concentration of carbon and nitrogen compared to the raw RDF pellet sample. This rise was more noticeable in the dry carbonization tests with an increase of 21.2%

 doi:10.20944/preprints202406.1905.v1

of carbon content for chars produced at 400°C. Additionally, there was a significant reduction in oxygen concentration and the absence of sulfur in the chars, which is a benefit of the dry carbonization process.

For chars, the concentration of carbon and nitrogen exhibits a marginal rise upon the addition of biomass compared to the sample consisting solely of RDF pellets. Hydrogen content showed a modest increase with a 10% biomass incorporation, then declines as biomass content reaches 25%, while sulfur was absent in all samples. The increase in carbon concentration associated with the decrease in hydrogen concentration reduces the H/C ratio of char and improves its fuel properties [37]. Oxygen content falls with a 10% biomass addition but escalates at 25%, predominantly due to the decreased hydrogen and ash quantities.

In hydrochars, the temperature increase did not affect the carbon concentration significantly, but it led to a slight increase in the nitrogen concentration. Regarding the increase in the S/L ratio, the carbon content showed an increase at 250°C, while it remained nearly constant at 300°C. However, the temperature rise caused a small reduction in the hydrogen content and an increase in the nitrogen and oxygen concentrations. Throughout all samples, the sulfur concentration accounted for 0.2% of the total.

Table 3. Elemental composition of the RDF pellet chars produced by dry and hydrothermal carbonization.

Sample	Elemental composition (%, daf)				
	C	H	N	S	O
Raw RDF	45.8 ± 1.9	5.9 ± 0.4	1.0 ± 0.2	0.1 ± 0.0	31.3 ± 2.5
LBW	49.4 ± 0.2	6.3 ± 0.1	0.9 ± 0.1	0.1 ± 0.0	37.1 ± 0.3
100P	55.5 ± 1.7	6.9 ± 0.3	1.5 ± 0.2	0.0 ± 0.0	9.8 ± 1.0
90P10B	60.0 ± 1.1	7.2 ± 0.2	1.7 ± 0.1	0.0 ± 0.0	6.2 ± 0.3
75P25B	61.7 ± 1.8	6.4 ± 0.3	1.7 ± 0.2	0.0 ± 0.0	8.5 ± 0.8
100P 250°C 1:2.5	47.8 ± 1.1	5.5 ± 0.2	1.5 ± 0.1	0.2 ± 0.0	20.4 ± 1.5
100P 250°C 1:5	49.6 ± 1.1	5.9 ± 0.2	1.3 ± 0.1	0.2 ± 0.0	21.9 ± 1.6
100P 300°C 1:2.5	49.7 ± 1.6	5.4 ± 0.3	1.7 ± 0.2	0.2 ±0.1	24.2 ± 1.2
100P 300°C 1:5	49.5 ± 1.3	5.3 ± 0.2	1.6 ± 0.1	0.2 ± 0.0	22.9 ± 1.5

The Van Krevelen diagram (Figure 3) indicates that the reduction in the O/C ratio was much more pronounced in char samples, with values similar to bituminous coal, while the reduction observed in hydrochars led to values closer to lignite. The incorporation of biomass in the samples was found to lower this ratio compared to the sample consisting only of RDF pellets, although a proportional reduction to the biomass addition was not observed, where the lowest value was in the sample with 10% biomass. In the case of hydrochars, the lowest S/L ratio demonstrated to have a greater influence than the carbonization temperature. The decrease in oxygen concentration is primarily caused by the dewatering, dehydration, and decarboxylation reactions that occur during both carbonization processes. However, these reactions were more noticeable in the dry carbonization experiments, possibly due to the higher temperature severity [38].

 doi:10.20944/preprints202406.1905.v1

In terms of the H/C ratio, the reduction was more subtle compared to the raw RDF. The increase in biomass content in chars was directly related to the reduction of this ratio, while in hydrochars, the increase in the S/L ratio had a greater impact on reducing the value. For all the chars and hydrochars produced, the H/C ratio ranged from 1.23 to 1.49, while for the raw RDF it was 1.53. This demonstrates a less noticeable reduction compared to the O/C ratio as observed in other studies [39].

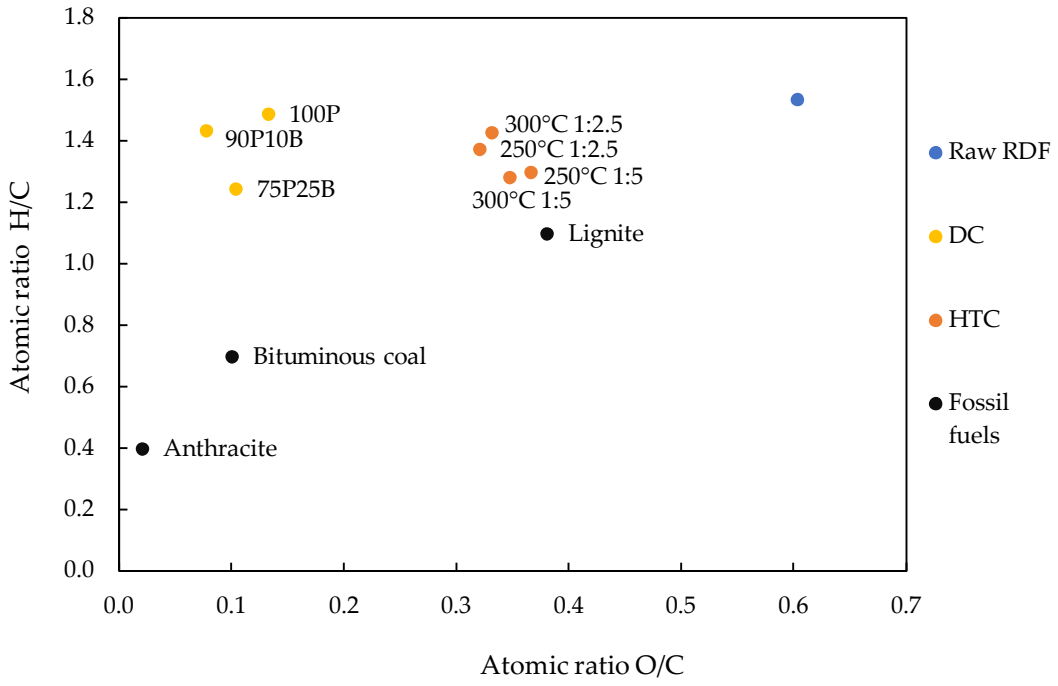

Figure 3. Van Krevelen diagram from the chars and hydrochars pellets.

The HHV of the chars is represented in Figure 4a. It has been observed that the incorporation of biomass does not significantly affect the HHV of chars. The HHV for pellet chars without biomass incorporation is 25.0 MJ/kg, and with 25% incorporation, it is 25.1 MJ/kg. However, the sample with 10% biomass showed a lower value of 23.6 MJ/kg. On the other hand, it has been found that the washing process is associated with an increase in the HHV of chars. In all conditions, the char exhibited a higher HHV value than the chars before the washing process.

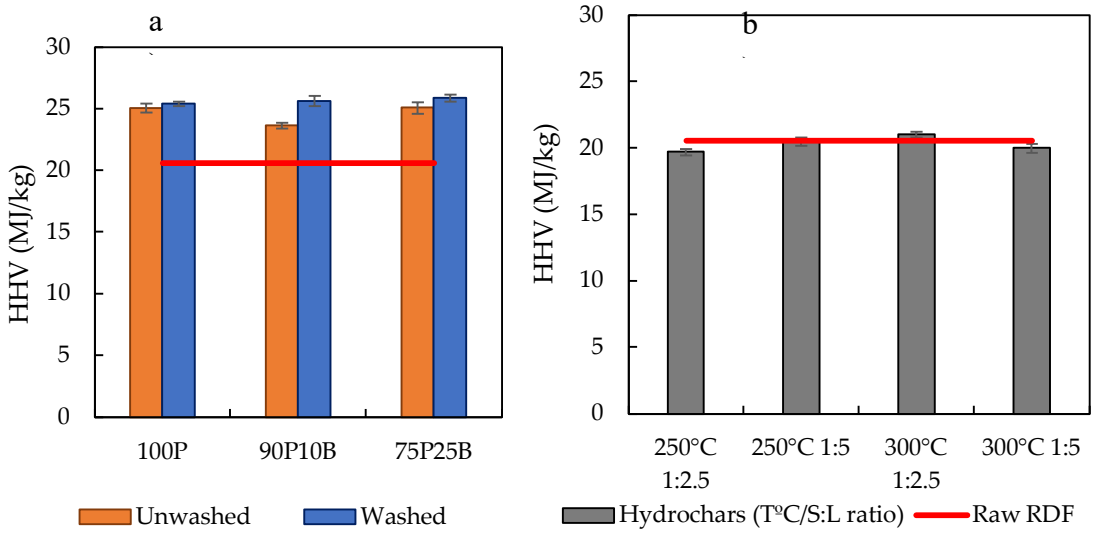

Figure 4. High heating value of the RDF pellet chars (a),and hydrochars (b).

 doi:10.20944/preprints202406.1905.v1

The increase in this parameter was gradual to the incorporation of biomass, where the highest value obtained was 25.9 MJ/kg in chars with 25% biomass. The sample composed only of RDF pellets presented a value of 25.4 MJ/kg, while in the sample with 10% biomass incorporation the value was 25.6 MJ/kg. The increase in HHV of chars after the washing process was also reported in previous work [34]. The HHV of hydrochars can be seen in Figure 4b. Increasing the temperature from 250°C to 300°C demonstrated an influence on the HHV of hydrochars produced at the S/L ratio of 1:2.5. At the lowest temperature, the HHV was 19.7 MJ/kg, while at 300°C this value was 21 MJ/kg. At the S/L ratio of 1:5, the HHV was slightly higher in the sample produced at 250°C (20.5 MJ/kg) when compared to the sample produced at 300°C (20.0 MJ/kg).

The composition of chars and hydrochars ashes is represented in Table 3. CaO and Al_2O_3 correspond to the largest fraction in all samples. The incorporation of biomass in a greater proportion caused a reduction in these components in relation to RDF pellets, however the addition of 10% demonstrated a slight increase.

Table 3. Ash mineral composition from the chars and hydrochars.

Ash mineral composition		**Dry carbonization**			**Hydrothermal carbonization**	
		100P	**90P10B**	**75P25B**	**100P 250°C/1:2.5**	**100P 300°C/1:2.5**
Oxides (%, w/w)	Al_2O_3	13.9	14.1	12.5	19.6	13.8
	CaO	30.8	32.6	29.4	35.6	22.1
	Fe_2O_3	5.4	4.3	3.7	4.8	3.1
	K_2O	3.2	3.4	3.3	1.3	0.8
	MgO	9.0	9.5	9.8	5.3	4.4
	Na_2O	1.8	1.9	1.9	0.8	0.5
	SiO_2	0.2	0.3	0.4	6.7	0.5
	TiO_2	0.6	0.6	0.7	0.3	0.2
Fouling and slagging index	B/A	3.4 h	3.4 h	3.5 h	1.8 h	2.1 h
	BAI	1.1 l	0.8 l	0.7 l	2.4 l	2.3 l
	Fu	7.5 h	7.6 h	7.6 h	0.1 l	0.4 l
	S/A	0.0 l	0.0 l	0.0 l	0.3 m	0.0 l
	TA	5.0 h	5.3 h	5.2 h	2.0 h	1.3 h
Chlorine (%)		0,4	0.4	0.4	1.0	1.1
Ash (%)		26,3	25.0	21.6	17.2	21.0

l - low; m - medium; h – high.

Apart from Fe_2O_3, which reduced its concentration with the incorporation of biomass, and K_2O, which remained at constant levels, the other elements showed an increase in relation to char produced only by RDF pellets. This increase was most evident in MgO concentrations, characteristic of the biomass composition [40]. In relation to hydrochars, the increase in the carbonization temperature led to the reduction of all analysed elements.

 doi:10.20944/preprints202406.1905.v1

The reduction of alkaline compounds such as K, Mg, and Na in hydrochars led to a reduction in the base/acid ratio (B/A) and, more significantly, in the fouling index (Fu). This reduction meant that these samples were categorized as having a low tendency to form scale (<0.4) compared to char samples. The agglomeration index (BAI) was low in all samples, with hydrochars showing a lower trend. A lower BAI value (<0.15) indicates a higher probability of agglomerate formation in the reactor bed. The tendency for slag formation (S/A) was low in all samples (<0.3), except for the hydrochar sample at 250°C, which fell within the medium trend category. The potential for the formation of ash layers (T/A) was high (>0.3) in all samples, but there was a significant reduction in hydrochars [32].

The chlorine content of the chars is represented in Figure 5a. Prior to the washing process, only the sample with the highest biomass incorporation had a value lower than 1% (0.9%). However, due to the heterogeneity of the RDF composition, variation in this value does not guarantee that this composition produces chars with chlorine contents within the permitted limit for use as an alternative fuel. After washing, the samples exhibited a significant reduction in this parameter, with the final concentration at around 0.4% for all three samples. This reduction ranged from 73.4% in the sample without biomass to 61.7% in the sample with the highest percentage of this fraction.

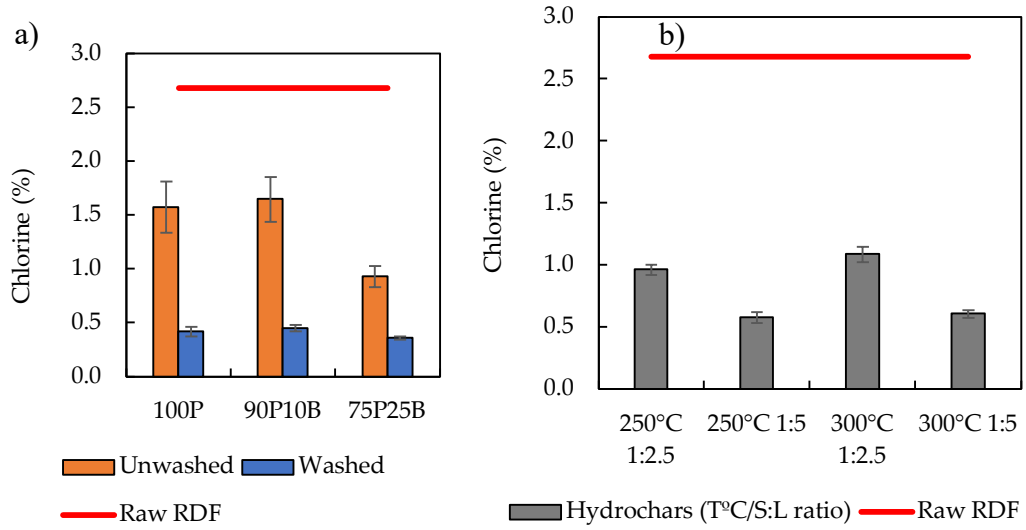

Figure 5. Chlorine content on the unwashed and washed chars (a), and hydrochars (b).

Figure 5b shows the chlorine content of hydrochars, where increasing the carbonization temperature demonstrated a slight increase in this parameter. Conversely, increasing the S/L ratio in the HTC process led to a significant reduction in chlorine content. At a temperature of 250°C, the increase in the S/L ratio represented a 39.6% reduction in chlorine content (0.6%) compared to the S/L ratio of 1:2.5 (1.0 %). Similarly, at a temperature of 300°C, the chlorine content decreased by 44% when the S/L ratio was increased from 1:2.5 to 1:5.

The thermogravimetric profile of chars and hydrochars can be seen in Figure 6. For chars, the most significant mass loss occurred between 235-540 °C, with a gradual reduction as the temperature increased (Figure 6a). Up to 235°C, the reduction ranged from 2.8-5.8%, with the sample composed solely of RDF pellets showing a greater reduction, likely due to the higher moisture content of the pellets compared to biomass. The temperature range where the greatest mass loss occurred represented between 65-66.4%, being proportionally higher with the increase in the incorporation of biomass, due to the high degradation of the components of this fraction (mainly hemicellulose and cellulose) in this temperature range [41]. In the sample with greater biomass incorporation, the temperature range of greater mass reduction extends to approximately 600°C.

Regarding the hydrochars, the mass loss up to 235°C was like that observed for pellet chars (5.1-5.4%) in samples produced at the S/L ratio of 1:2.5. However, increasing the ratio to 1:5 resulted in a smaller mass reduction up to this temperature (3.8%). The chars produced by HTC exhibited greater

 doi:10.20944/preprints202406.1905.v1

thermal resistance, as the mass reduction was lower in the temperature range observed in the chars, and at 540°C the mass loss was 57.5-61% (Figure 6b). Furthermore, the temperature at which mass loss stability occurred was higher when compared to chars produced from dry carbonization (~ 600°C).

The thermal differential graphs indicate that there is an initial peak of greater mass reduction up to 150°C, which is attributed to water loss. This is more noticeable in chars (see Figure 6c) due to their higher moisture content. The highest peak of thermal degradation starts at 200°C and extends up to 440°C, being more evident in the sample with 10% biomass incorporation. Although the sample with the highest percentage of biomass exhibited a smaller peak in this temperature range, it was broader and extended over a greater temperature range. A similar behavior was observed in the second peak of maximum degradation, between 700 and 780°C, which was more noticeable at the lowest temperature in the sample with 10% biomass.

Figure 6d shows the thermal degradation rate of hydrochars. The largest peak occurred at temperatures close to that observed in chars (around 420°C). However, there is a prominent peak between 270-325°C, which may be related to the higher devolatilization of hydrochars due to their higher volatile matter content. This peak was more pronounced in the sample with the highest volatile content (250°C, S/L 1:5), being higher than the peak observed at the temperature of greatest degradation, and less noticeable in samples produced at 300°C. In contrast to chars, two other peaks of greater degradation of hydrochars were observed, one between 600-650°C and the other between 700-780°C.

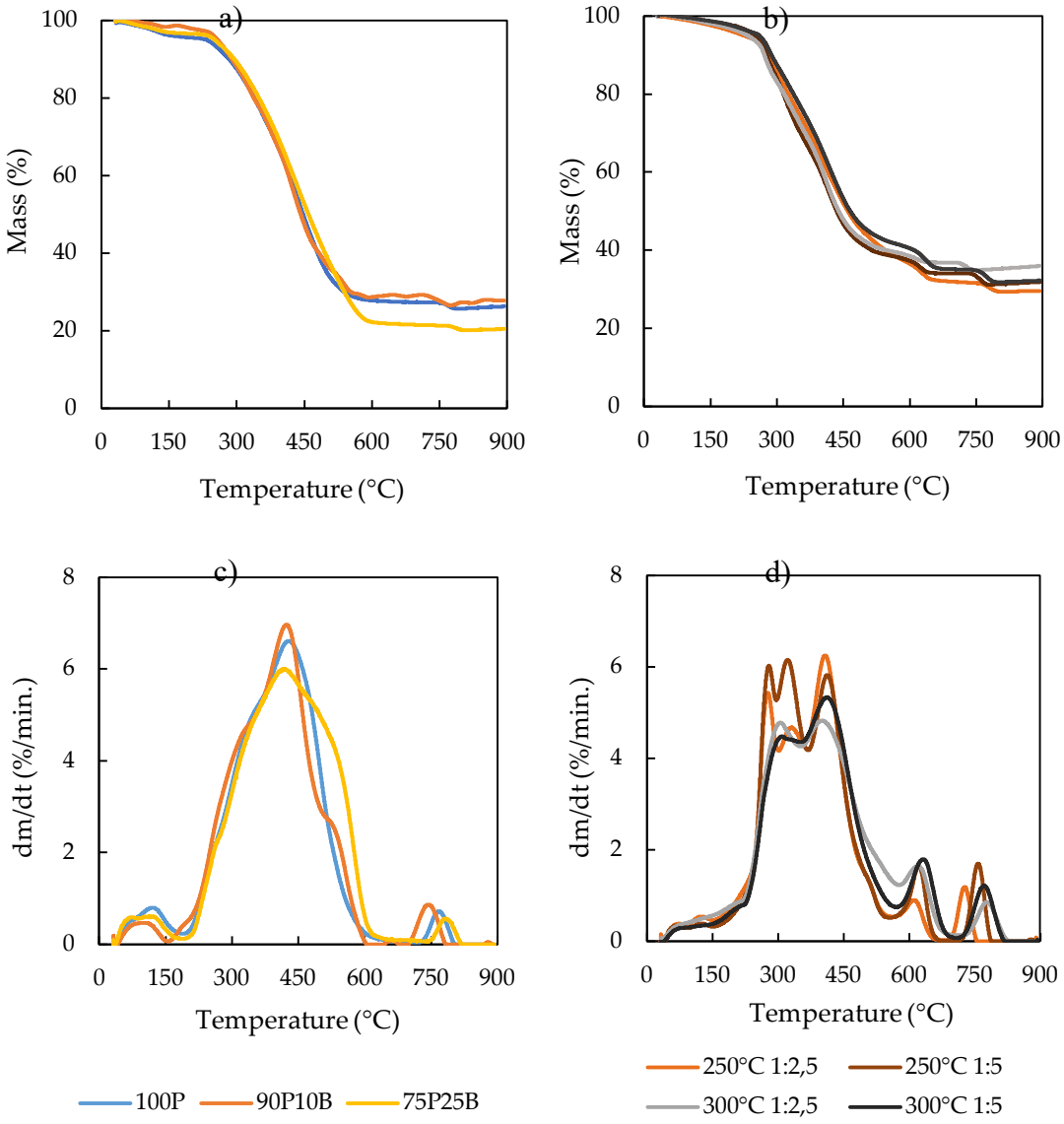

 doi:10.20944/preprints202406.1905.v1

Figure 6. Thermogravimetric profile of the chars (a, c), and hydrochars (b, d) of RDF pellets.

The ignition and burnout temperatures were estimated according to the intercepted method, and the results are represented in Table 4. The maximum degradation temperatures and the degradation rate in the two main peaks observed in the DTG are also presented. The addition of biomass into RDF pellets in chars demonstrated little influence on Ti and Tb, although there was a slight increase in the sample with a higher percentage of this fraction. Conversely, hydrothermal carbonization seems to influence the reduction of Ti and increase Tb, except for hydrochar at 250°C at the lowest S/L ratio. It is important to note that a decrease in Ti increases the risks of auto-ignition of chars during storage and transportation [42], while an increase in Tb requires higher temperatures for complete degradation [43] during admission to gasifiers, for example.

Table 4. Thermal degradation behaviour of the chars and hydrochars from RDF pellets.

Sample	T_i (°C)	T_b (°C)	T_1 (°C)	T_2 (°C)	DTG1 (%/min.)	DTG2 (%/min.)
100P	332	765	441	769	6.6	0.7
90P10B	332	760	422	745	7.0	0.9
75P25B	337	766	418	782	6.0	0.5
100P 250 1:2,5	299	732	408	727	6.2	1.2
100P 250 1:5	310	850	324	757	6.1	1.7
100P 300 1:2,5	288	796	408	776	4.8	0.9
100P 300 1:5	300	798	422	764	5.3	1.2

The FTIR profiles of the chars produced only from RDF pellets and with 25% biomass incorporation, in addition to the hydrochars produced at 250 and 300°C in an S/L ratio of 1:2.5 can be seen in Figure 7.

The band between 3429-3376 cm^{-1}, which corresponds to the stretching of O-H bonds, was more noticeable in the samples composed only of RDF pellets, while in the char sample with biomass incorporation this band was more discreet, representing the largest elimination of these elements as demonstrated in the Van Krevelen diagram.

 doi:10.20944/preprints202406.1905.v1

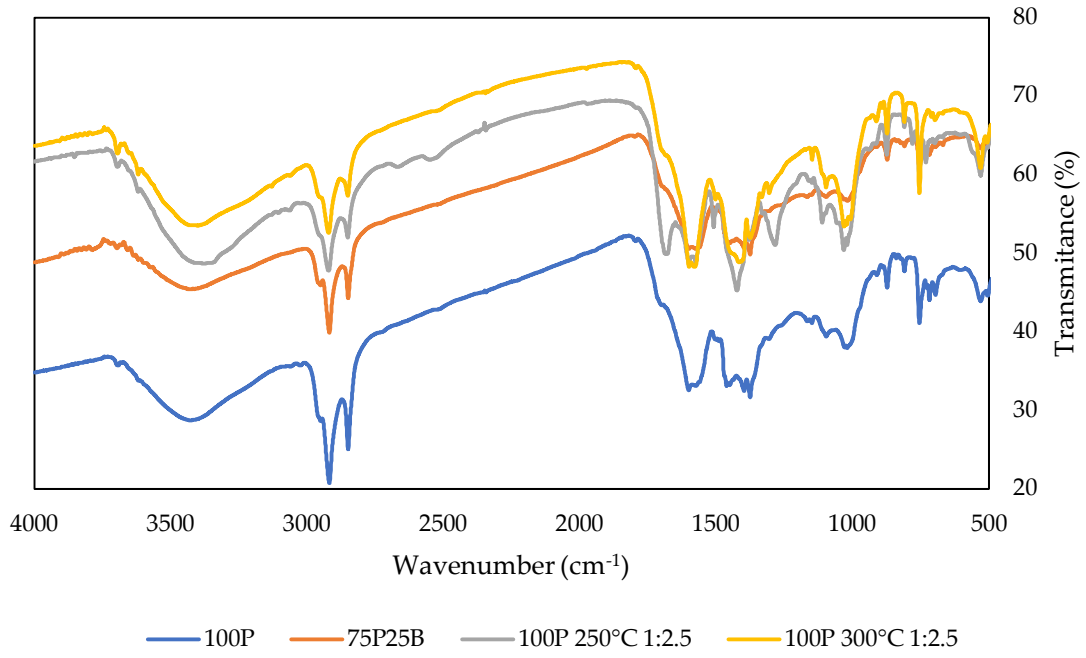

Figure 7. FTIR spectrum from the chars and hydrochars.

The bands observed between 2951-2849 cm^{-1}, attributed to stretching vibrations of the C-H bonds, were observed in all samples, being more evident in chars, especially in those produced from 100% RDF pellets. A greater number of bands between 1600-1200 cm^{-1} in the hydrochars samples, as well as a more pronounced band at 755 cm^{-1}, suggests a greater degree of aromaticity of these chars [18].

3.2. Effluents Characterization

The characterization of the char washing wastewater and the liquid effluent of the HTC process is represented in Table 5. The pH of the char washing wastewater presented a neutral character without significant variations with the incorporation of biomass (6.7-6.8), while the HTC liquid presented an acidic pH (4.8-5.0) characteristic of these effluents [44].

Table 5. Characterization of wastewater from chars washing process and HTC effluents.

Analysis	Samples						
	DC			HTC			
	100P	90P10B	75P25B	100P 250/1:2,5	100P 250/1:5	100P 300/1:2,5	100P 300/1:5
pH	6.8	6.8	6.7	4.8	4.8	4.8	5.0
COD (g/L)	4.3	3.4	4.5	61.0	37.3	60.4	37.1
Chlorides (mg/L)	1.8	1.9	1.3	4.1	2.1	5.6	2.5
Total solids (g/L)	8.3	8.1	7.7	41.8	14.8	43.4	11.9
Volatile solids (g/L)	4.4	4.1	4.4	31.2	11.4	24.7	8.7

 doi:10.20944/preprints202406.1905.v1

Fixed solids (g/L)		3.9	3.9	3.3	10.6	3.4	18.7	3.2
Ash mineral composition (w/w%, db)	Al_2O_3	0.4	0.5	2.7	0.4	0.2	0.6	0.1
	CaO	25.3	20.5	23.1	32.4	15.8	21.4	17.3
	Fe_2O_3	0.2	0.1	0.3	2.6	1.1	0.3	0.1
	K_2O	22.5	22.1	23.6	22.0	6.7	18.0	9.3
	MgO	4.8	4.7	6.6	16.8	2.4	17.9	1.3
	Na_2O	17.6	14.1	17.2	12.7	11.7	11.1	7.4
	SiO_2	0.9	1.3	6.0	2.3	2.6	3.3	2.4
	TiO_2	0.0	0.0	0.0	0.0	0.0	0.0	0.0

Regarding COD, no characteristic pattern was observed in the char washing wastewaters, varying from 3.4 to 4.5 g/L. Very high values of this parameter were observed in HTC effluents, mainly in those produced during carbonization at the S/L ratio of 1:2.5. The increase in temperature did not demonstrate a significant influence, being slightly lower in tests at 300°C. On the other hand, increasing the S/L ratio to 1:5 was responsible for the 39% reduction in COD values in both samples. The same can be observed in the values of chlorides and total solids in the samples. The increase in the S/L ratio led to a reduction between 48 and 55% in the chloride content, while the reduction in total solids varied between 65 and 73%.

Regarding the mineral composition of the ash, a gradual increase in the concentration of Al oxides (0.4-2.7%), Mg (4.8-6.6%) and Si (0.9-6. 0%) in char washing wastewater with increased biomass incorporation. In the case of HTC effluents, increasing the S/L ratio from 1:2.5 to 1:5 demonstrated a significant reduction in all analysed elements, except for Si at a temperature of 250°C.

4. Conclusion

The carbonization of RDF pellets has been found to be effective in producing chars with improved combustible properties compared to raw residue. Dry carbonization tests show that the RDF pellets have a greater tendency to agglomerate compared to the fluff form. Therefore, incorporating biomass waste in the form of sawdust can be an alternative to minimize this issue. Adding 10% and 25% of biomass to RDF pellets resulted in the production of chars with fewer agglomerates that are more susceptible to the crushing process. Additionally, the incorporation of biomass in carbonization at 400°C reduced the O/C and H/C ratios as well as the ash content (- 5.3 – 17.9%), while slightly increasing the calorific value of chars (+2%). However, the increase in the percentage of biomass in the sample reduced the mass yield (- 4.5%) and decreased the apparent density of chars (-6.6%). Tests have shown that RDF pellets are more susceptible to self-ignition, with combustion occurring in most tests when the temperature is raised above 400°C. Regarding hydrothermal carbonization, the S/L ratio of 1:2.5 was not enough to reduce the chlorine content to values below 1%. This would not justify the application of this thermochemical method, as a washing step would be needed to reduce this value. Considering the hydrochars produced at the S/L ratio of 1:5, increasing the temperature to 300°C reduced the mass yield by 8.9% while increasing the apparent density by 8.1%. Hydrochars exhibited lower Ti and higher Tb compared to chars. Furthermore, the increase in temperature reduced the formation of agglomerates in hydrochars, resulting in reduced crushing costs and improved combustion and gasification efficiency. In summary, the dry carbonization of RDF pellets with 10% sawdust incorporation appears as a viable alternative to increase the HHV of chars, reduce the formation of agglomerates, and minimize the risk of self-ignition during the process.

 doi:10.20944/preprints202406.1905.v1

Author Contributions: Conceptualization, A.L. and M.G.; formal analysis, A.L., R.P.; N.P.; resources, C.V. and P.B.; data curation, A.L.; validation: A.L.; writing—original draft preparation, A.L.; writing—review and editing, A.L., N.P., P.B.; supervision, M.G. and P.B. All authors have read and agreed to the published version of the manuscript.

Funding: This work was co-funded by: Compete 2020, Portugal 2020, and the European Union through the European Regional Development Fund—FEDER within the scope of the project AmbWTE: Biomass & Waste to Energy System project (POCI-01-0247-FEDER-039838); Fundação para a Ciência e Tecnologia, I.P. (Portuguese Foundation for Science and Technology), under projects UIDB/05064/2020 (VALORIZA - Research Centre for Endogenous Resource Valorization), UIDB/04077/2020-2023 and UIDP/04077/2020-2023 (MEtRICs - Mechanical Engineering and Resource Sustainability Center); Alentejo2020 (Regional Operational Program of Alentejo), grant no. ALT20-05-3559-FSE-000035.

Data Availability Statement: The data presented in this study are available on request from the corresponding authors.

Conflicts of Interest: The authors declare no conflicts of interest.

References

1. Alam, S.; Rokonuzzaman, M.; Rahman, K.S.; Haque, A.; Chowdhury, S.; Prasetya, T.A.E. Techno-economic and environmental analysis of organic municipal solid waste for energy production. *Heliyon*, **2024**, 10(11) e31670. doi: 10.1016/j.heliyon.2024.e31670.
2. Wang, X., Li, C., Lam, C.H., Subramanian, K., Qin, Z-H., Mou, J-H., Jin, M., Chopra, S.S:, Singh, V., Ok, Y.S:, Yan, J., Li, H-Y., Lin, C.S.K. Emerging waste valorisation techniques to moderate the hazardous impacts, and their path towards sustainability. *J. Hazard. Mater*. **2022**, 423, 127023. doi: 10.1016/j.jhazmat.2021.127023.
3. Mong, G.R., Tan, H., Sheng, D.D.C.V., Kek, H.Y., Nyakuma, B.B., Woon, K.S., Othman, M.H.D., Kang, H.S., Goh, P.S., Wong, K.Y. A review on plastic waste valorisation to advanced materials: Solutions and technologies to curb plastic waste pollution. *J. Clean. Prod.* **2024**, 434, 140180. doi: 10.1016/j.jclepro.2023.140180.
4. Said, Z., Sharma, P., Nhuong, Q.T.B., Bora, B.J., Lichtfouse, E., Khalid, H.M., Luque, R., Nguyen, X.P., Hoang, A.T. Intelligent approaches for sustainable management and valorisation of food waste. *Bioresour. Technol*. **2023**, 377, 128952. doi: 10.1016/j.biortech.2023.128952.
5. J. Hong, J., Chen, Y., Wang, M., Ye, L., Qi, C., Yuan, H., Zheng, T., Li, X. Intensification of municipal solid waste disposal in China. *Renew. Sustain. Energy Rev.* **2017**, 69, 168–176. doi: 10.1016/j.rser.2016.11.185.
6. Santos, S.M.; Nobre, C.; Brito, P.; Gonçalves, M. Brief Overview of Refuse-Derived Fuel Production and Energetic Valorization: Applied Technology and Main Challenges. *Sustain.*, **2023**, 15(13). doi: 10.3390/su151310342.
7. Tihin, G.L., Mo, K.H.; Onn, C.C.; Ong, H.C.; Taufiq-Yap, Y.H.; Lee, H.V. Overview of municipal solid wastes-derived refuse-derived fuels for cement co-processing. *Alexandria Eng. J.* **2023**, 84, 153–174. doi: 10.1016/j.aej.2023.10.043.
8. Guo, M., Wang, K., Bing, X., Cheng, J., Zhang, Y., Sun, X., Guan, B., Yu, J. Pyrolysis of plastics-free refuse derived fuel derived from municipal solid waste and combustion of the char products in lab and pilot scales: A comparative study. *Fuel* **2024**, 359, 130335. doi: 10.1016/j.fuel.2023.130335.
9. Domínguez, J.I., Blanco Machín, E., Travieso Pedroso, D., Wagemman Herrera, E., Cuevas Barraza, C. Advanced thermoconversion technology for municipal solid waste energetic valorization. *Renew. Energy* **2024**, 228, 120604. doi: 10.1016/j.renene.2024.120604.
10. Chen, S., Liu, Z., Jiang, S., Hou, H. Carbonization: A feasible route for reutilization of plastic wastes. *Sci. Total Environ.* **2020**, 710, 136250. doi: 10.1016/j.scitotenv.2019.136250.
11. Bardhan, M., Novera, T.M., Tabassum, M., Islam, M.A., Islam, M.A., Hameed, B.H. Co-hydrothermal carbonization of different feedstocks to hydrochar as potential energy for the future world: A review. *J. Clean. Prod*. **2021**, 298. doi: 10.1016/j.jclepro.2021.126734.
12. Lin, Y., Ge, Y., Xiao, H., He, Q., Wang, W., Chen, B. Investigation of hydrothermal co-carbonization of waste textile with waste wood, waste paper and waste food from typical municipal solid wastes. *Energy* **2020**, 210. doi: 10.1016/j.energy.2020.118606.
13. He, C., Zhang, Z., Ge, C., Liu, W., Tang, Y., Zhunag, X., Qiu, R. Synergistic effect of hydrothermal co-carbonization of sewage sludge with fruit and agricultural wastes on hydrochar fuel quality and combustion behavior. *Waste Manag.* **2019**, 100, 171–181. doi: 10.1016/j.wasman.2019.09.018.
14. Li, Q., Lin, H., Zhang, S., Yuan, X., Gholizadeh, M., Wang, Y., Xiang, J., Hu, S., Hu, X. Co-hydrothermal carbonization of swine manure and cellulose: Influence of mutual interaction of intermediates on properties of the products. *Sci. Total Environ.* **2021**, 791, 148134. doi: 10.1016/j.scitotenv.2021.148134.

15. Dong, X., Wang, Z., Zhang, J., Zhan, W., Gao, L., He, Z. Synthesis and characteristics of carbon-based synfuel from biomass and coal powder by synergistic co-carbonization technology. *Renew. Energy* **2024**, 227, 120458. doi: 10.1016/j.renene.2024.120458.
16. Rago, Y.P., Collard, F.X., Görgens, J.F., Surroop, D., Mohee, R. Torrefaction of biomass and plastic from municipal solid waste streams and their blends: Evaluation of interactive effects. *Fuel* **2020**, 277. doi: 10.1016/j.fuel.2020.118089.
17. Shen, Y., Yu, S. Ge, S., Chen, X. Ge, X., Chen, M. Hydrothermal carbonization of medical wastes and lignocellulosic biomass for solid fuel production from lab-scale to pilot-scale. *Energy* **2017**, 118, 312–323. doi: 10.1016/j.energy.2016.12.047.
18. Yao, Z., Ma, X. Characteristics of co-hydrothermal carbonization on polyvinyl chloride wastes with bamboo. *Bioresour. Technol.* **2018**, 247, 302–309. doi: 10.1016/j.biortech.2017.09.098.
19. Brand, M.A., Mariano Rodrigues, T., Peretti da Silva, J., Oliveira, J. Recovery of agricultural and wood wastes: The effect of biomass blends on the quality of pellets. *Fuel* **2021**, 284. doi: 10.1016/j.fuel.2020.118881.
20. Yang, Y., Sun, M. Zhang, M., Zhang, K., Wang, D., Lei, C. A fundamental research on synchronized torrefaction and pelleting of biomass. *Renew. Energy* **2019**, 142, 668–676.doi: 10.1016/j.renene.2019.04.112.
21. Kaliyan, N., Vance Morey, R. Factors affecting strength and durability of densified biomass products. *Biomass and Bioenergy* **2009**, 33(3) 337–359. doi: 10.1016/j.biombioe.2008.08.005.
22. Sprenger, C.J., Tabil, L. G., Soleimani, M., Agnew, J., Harrison, A. Pelletization of refuse-derived fuel fluff to produce high quality feedstock. *J. Energy Resour. Technol. Trans. ASME* **2018**, 140(4). doi: 10.1115/1.4039315.
23. Zaini, I.N., Wen, Y., Mousa, E., Jönsson, P.G., Yang, W. Primary fragmentation behavior of refuse derived fuel pellets during rapid pyrolysis. *Fuel Process. Technol.* **2021**, 216. doi: 10.1016/j.fuproc.2021.106796.
24. García, R., González-Vázquez, M.P., Rubiera, F., Pevida, C., Gil, M.V. Co-pelletization of pine sawdust and refused derived fuel (RDF) to high-quality waste-derived pellets. *J. Clean. Prod.* **2021**, 328. doi: 10.1016/j.jclepro.2021.129635.
25. Rezaei, H., Yazdanpanah, F., Lim, C.J., Sokhansanj, S. Pelletization properties of refuse-derived fuel - Effects of particle size and moisture content. *Fuel Process. Technol.* **2020**, 205. doi: 10.1016/j.fuproc.2020.106437.
26. Surup, G.R., Leahy, J.J., Timko, M.T., Trubetskaya, A. Hydrothermal carbonization of olive wastes to produce renewable, binder-free pellets for use as metallurgical reducing agents. *Renew. Energy* **2020**, 155, 347–357. doi: 10.1016/j.renene.2020.03.112.
27. Cao, Z., Zhang, S., X., Liu, H., Sun, M., Lyu, J. Correlations between the compressive strength of the hydrochar pellets and the chemical components: Evolution and densification mechanism. *J. Anal. Appl. Pyrolysis* **2020**, 152. doi: 10.1016/j.jaap.2020.104956.
28. Sharma, H.B., Dubey, B.K. Binderless fuel pellets from hydrothermal carbonization of municipal yard waste: Effect of severity factor on the hydrochar pellets properties. *J. Clean. Prod.* **2020**, 277. doi: 10.1016/j.jclepro.2020.124295.
29. Sharma, H.B., Dubey, B.K. Co-hydrothermal carbonization of food waste with yard waste for solid biofuel production: Hydrochar characterization and its pelletization. *Waste Manag.* **2020**, 118, 521–533. doi: 10.1016/j.wasman.2020.09.009.
30. Jewiarz, M., Mudryk, K., Wróbel, M., Fraczek, J., Dziedzic, K. Parameters affecting RDF-based pellet quality. *Energies* **2020**, 13(4). doi: 10.3390/en13040910.
31. Nasiri, S., Hajinezhad, A., Kianmehr, M.H., Tajik, S. Enhancing municipal solid waste efficiency through Refuse Derived Fuel pellets: Additive analysis, die retention time, and temperature impact. *Energy Reports* **2023**, 10, 941–957. doi: 10.1016/j.egyr.2023.07.039.
32. Ovčačíková, H., Velička, M., Vlček, J., Topinková, M., Klárová, M., Burda, J. Corrosive Effect of Wood Ash Produced by Biomass Combustion on Refractory Materials in a Binary Al–Si System. *Materials (Basel).* **2022**, 15(16). doi: 10.3390/ma15165796.
33. Liu, X., Tan, H., Wang, X., Wang, Z., Xiong, X. Oxidation reactivity and kinetic analysis of bituminous coal char from high-temperature pyrolysis: Effect of heating rate and pyrolysis temperature. *Thermochim. Acta* **2020**, 690. doi: 10.1016/j.tca.2020.178660.
34. Longo, A., Sen, A.U., Nobre, C., Brito, P., Gonçalves, M. Dry and Hydrothermal Co-Carbonization of Mixed Refuse-Derived Fuel (RDF) for Solid Fuel Production. *Reactions* **2024**, 5, 77–97. doi: /10.3390/ reactions5010003.
35. Kambo, H.S., Dutta, A. Comparative evaluation of torrefaction and hydrothermal carbonization of lignocellulosic biomass for the production of solid biofuel. *Energy Convers. Manag.* **2015**, 105, 746–755. doi: 10.1016/j.enconman.2015.08.031.
36. Verhoeff, F., Adell i Arnuelos, A., Boersma, A.R., Pels, J.R., Lensselink, J., Kiel, J.H.A., Schukken, H. TorTech Torrefaction Technology for the production of solid bioenergy carriers from biomass and waste. *Energy Research Centre of the Netherlands* **2011**, 82pp.

37. Chen, W.H., Lu, K.M., Tsai, C.M. An experimental analysis on property and structure variations of agricultural wastes undergoing torrefaction. *Appl. Energy* **2012**, 100, 318–325. doi: 10.1016/j.apenergy.2012.05.056.
38. Kim, D., Park, K.Y., Yoshikawa, K. Conversion of Municipal Solid Wastes into Biochar through Hydrothermal Carbonization. *Eng. Appl. Biochar* **2017**, 31-46. doi: 10.5772/intechopen.68221.
39. Alves, O., Nobre, C., Durão, L., Monteiro, E., Brito, P., Gonçalves, M. Effects of dry and hydrothermal carbonisation on the properties of solid recovered fuels from construction and municipal solid wastes. *Energy Convers. Manag.* **2021**, 237. doi: 10.1016/j.enconman.2021.114101.
40. Vassilev, S.V., Baxter, D., Andersen, L.K., Vassileva, C.G. An overview of the chemical composition of biomass. *Fuel* **2010**, 89(5), 913–933. doi: 10.1016/j.fuel.2009.10.022.
41. Li, M-F., Chen, L-X., Li, X., Chen, C-Z., Lai, Y-C., Xiao, X., Wu, Y-Y. Evaluation of the structure and fuel properties of lignocelluloses through carbon dioxide torrefaction. *Energy Convers. Manag.* **2016**, 119, 463–472. doi: 10.1016/j.enconman.2016.04.064.
42. Bach, Q.V., Skreiberg, O. Upgrading biomass fuels via wet torrefaction: A review and comparison with dry torrefaction. *Renew. Sustain. Energy Rev.* **2016**, 54, 665–677. doi: 10.1016/j.rser.2015.10.014.
43. Mota-Panizio, R., Hermoso-Orzáez, M.J., Carmo-Calado, L., Calado, H., Goncalves, M., Brito, P. Co-carbonization of a mixture of waste insulation electric cables (WIEC) and lignocellulosic waste, for the removal of chlorine: Biochar properties and their behaviors. *Fuel* **2022**, 320. doi: 10.1016/j.fuel.2022.123932.
44. Nobre, C., Alves, O., Durão, L., Şen, A., Vilarinho, C., Gonçalves, M. Characterization of hydrochar and process water from the hydrothermal carbonization of Refuse Derived Fuel. *Waste Manag.* **2021**, 120, 303–313. doi: 10.1016/j.wasman.2020.11.040.